

## Crystal Structure of a Complex between the *Actinomadura* R39 DD-Peptidase and a Peptidoglycan-mimetic Boronate Inhibitor: Interpretation of a Transition State Analogue in Terms of Catalytic Mechanism<sup>†</sup>

Liudmila Dzhekieva,<sup>‡,||</sup> Mathieu Rocaboy,<sup>§,||</sup> Frédéric Kerff,<sup>§</sup> Paulette Charlier,<sup>§</sup> Eric Sauvage,<sup>§</sup> and R. F. Pratt<sup>\*,‡</sup>

<sup>‡</sup>Department of Chemistry, Wesleyan University, Lawn Avenue, Middletown, Connecticut 06459, and <sup>§</sup>Centre d'Ingénierie des Protéines, Université de Liège, B-4000 Sart Tilman, Liège, Belgium. <sup>||</sup>Contributed equally to this work.

Received May 12, 2010; Revised Manuscript Received June 14, 2010

**ABSTRACT:** The *Actinomadura* R39 DD-peptidase is a bacterial low molecular weight class C penicillin-binding protein. It has previously been shown to catalyze hydrolysis and aminolysis of small D-alanyl-D-alanine terminating peptides, especially those with a side chain that mimics the amino terminus of the stem peptide precursor to the bacterial cell wall. This paper describes the synthesis of (D- $\alpha$ -aminopimelylamino)-D-1-ethylboronic acid, designed to be a peptidoglycan-mimetic transition state analogue inhibitor of the R39 DD-peptidase. The boronate was found to be a potent inhibitor of the peptidase with a  $K_i$  value of  $32 \pm 6$  nM. Since it binds some 30 times more strongly than the analogous peptide substrate, the boronate may well be a transition state analogue. A crystal structure of the inhibitory complex shows the boronate covalently bound to the nucleophilic active site Ser 49. The aminopimelyl side chain is bound into the site previously identified as specific for this moiety. One boronate oxygen is held in the oxyanion hole; the other, occupying the leaving group site of acylation or the nucleophile site of deacylation, appears to be hydrogen-bonded to the hydroxyl group of Ser 298. The Ser 49 oxygen appears to be hydrogen bonded to Lys 52. If it is assumed that this structure does resemble a high-energy tetrahedral intermediate in catalysis, it seems likely that Ser 298 participates as part of a proton transfer chain initiated by Lys 52 or Lys 410 as the primary proton donor/acceptor. The structure, therefore, supports a particular class of mechanism that employs this proton transfer device.

The bacterial DD-peptidases are a component of the metabolic pathway leading to the bacterial cell wall. There they catalyze the final steps of cell wall synthesis, incorporation of the stem peptide monomer into polymeric peptidoglycan, and sculpting of the final structure (1). From a human clinical standpoint, these enzymes are important as a target for antibiotics, i.e., antibacterial drugs. They are inhibited, for example, by the important  $\beta$ -lactam class of antibiotics and remain as a well-validated option for further antibiotic design (2). Scheme 1 shows the reactions catalyzed by these enzymes and the reaction leading to their inhibition by  $\beta$ -lactams. The reactions shown include transpeptidation, which extends the peptidoglycan polymer, and carboxypeptidation and endopeptidation, both of which lead to reduced cross-linking of the polymer.

Largely because of their relevance to the  $\beta$ -lactam antibiotics, these enzymes have been closely studied for many years (3–5). They have been classified into two groups, the

low molecular weight (LMW)<sup>1</sup> and high molecular weight (HMW) classes (5). The latter is further subdivided into two major groups, A and B, and the former into three groups, A, B, and C. This classification was initially based on molecular weight and amino acid sequence. Over the last 15 years, crystal structures of members of all of these classes have been obtained (6, 7). It is now clear that the classification relates directly to protein structure and, most likely therefore, to some degree at least, to function *in vivo*.

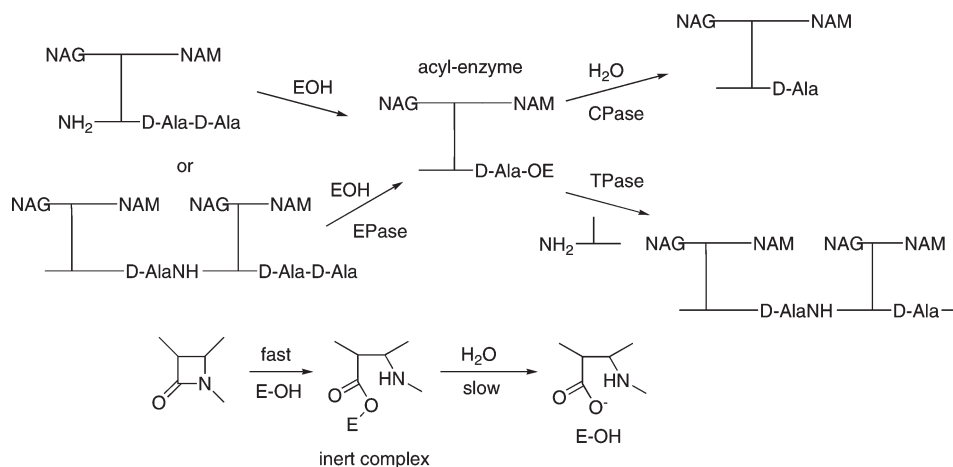
Although it seems clear that these enzymes must catalyze the reactions of Scheme 1 *in vivo*, their activity as DD-peptidases *in vitro* is less well characterized. To date, no strong affinity has been demonstrated between any HMW or LMWA enzymes and any specific elements of peptidoglycan structure, i.e., small peptides of structure based on that of the relevant peptidoglycan (8, 9). Such specificity, however, has been established for certain members of the LMWB and LMWC classes. For example, it is evident from peptide specificity studies and subsequent crystal structures that the *Streptomyces* R61 DD-peptidase (LMWB) has strong affinity for motif 1 (10–12) and that the *Actinomadura*

<sup>†</sup>This research was supported by National Institutes of Health Grant AI-17986 (R.F.P.) and in part by the Belgian Program on Interuniversity Poles of Attraction initiated by the Belgian State, Prime Minister's Office, Science Policy programming (IAP no. P6/19), the Fonds de la Recherche Scientifique (IISN4.4505.00, IISN4.4509.09, FRFC2.4.508.01.F, FRFC9.4.538.03.F, FRFC2.4.524.03), and the University of Liège (Fonds spéciaux, Crédit classique, 2009). F.K. is Chargé de Recherche of the Fonds de la Recherche Scientifique (F.R.S.-FNRS, Brussels, Belgium).

\*Corresponding author. Telephone: 860-685-2629. E-mail: rpratt@wesleyan.edu. Fax: 860-685-2211.

<sup>1</sup>Abbreviations: DIBAL, diisobutylaluminum hydride; DIPEA, diisopropylethylamine; DMF, dimethylformamide; ESMS, electrospray ionization mass spectroscopy; HATU, *O*-(7-azabenzotriazol-1-yl)-*N,N,N',N'*-tetramethyluronium hexafluorophosphate; HMW, high molecular weight; LMW, low molecular weight; MES, 4-morpholinoethanesulfonic acid; MOPS, 3-morpholinopropanesulfonic acid; NMR, nuclear magnetic resonance; PBP, penicillin-binding protein; THF, tetrahydrofuran.

Scheme 1



R39 DD-peptidase (LMWC) strongly interacts with motif **2** (13). These motifs are direct mimics of the stem peptides from the respective *Streptomyces* and *Actinomadura* organisms.

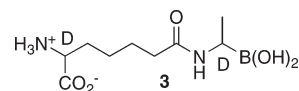


In each of these enzymes, therefore, it seems very likely that the dominant substrates *in vivo* also contain these structural elements; i.e., the substrates have a non-cross-linked N-terminus. These could be either monomers (carboxypeptidase activity) or oligomers/polymers (endopeptidase activity). The low micromolar  $K_m$  values of these specific substrates (10–13) suggest that structures such as **1** and **2** would be tightly trapped and processed by these enzymes *in vivo*.

The detailed mechanism of action of these enzymes has also been discussed at some length (6, 14–24). Much of the discussion has been based on the more developed state of  $\beta$ -lactamase mechanisms. This is rational since the active site structure of DD-peptidases is closely analogous to that of the serine  $\beta$ -lactamases because the latter enzymes are almost certainly evolutionary descendants of the former (25, 26). The active sites of HMWA, HMWB, LMWA, and LMWC DD-peptidases are closely analogous to that of a class A  $\beta$ -lactamase, although Glu 166, recruited to catalyze  $\beta$ -lactam-derived acyl-enzyme hydrolysis in the  $\beta$ -lactamase, is absent in the DD-peptidases. Since Glu 166 probably also participates in acylation (27–31), it is evident that both acylation and deacylation may be different in DD-peptidases than in  $\beta$ -lactamases.

One source of mechanistic information, and one that was rather extensively employed with  $\beta$ -lactamases, is that of the structure of transition state analogues. Typically, these are structures of the  $\beta$ -lactamase complexed to inhibitors that form anionic tetrahedral structures covalently bound to the nucleophilic active site serine residue and which mimic the high-energy tetrahedral intermediates/transition states of acyl transfer turnover. Important examples are those generated from boronates (32–34) and phosphonates (35–37). To date, phosphonates have not yielded any potent DD-peptidase inhibitors, although a weakly inhibitory phosphonate was employed to obtain a transition state analogue structure with the LMWB *Streptomyces* R61 DD-peptidase (38). Boronates, however, have shown promise of stronger inhibition. A peptide boronate has been shown to inhibit *Escherichia coli* PBP5 with a dissociation constant of 13  $\mu$ M (18), and more

recently, a variety of aryl boronates were found to inhibit the LMWC DD-peptidase of *Actinomadura* R39 (39). A crystal structure of a complex of the peptide boronate was interpreted in terms of a transition state analogue (18), but this interpretation is compromised somewhat by the nonspecific nature of the peptide moiety (the molecule is not a close peptidoglycan-mimetic and a large part of its peptide structure is not observed in the crystal structure) and the (resulting?) lack of contact of Ser 110 (equivalent to Ser 298 of the R39 enzyme) with the boronate moiety. In this paper, we describe **3**, a specific peptidoglycan-mimetic boronate inhibitor of the *Actinomadura* R39 DD-peptidase, with a thermodynamic inhibition constant of 32 nM. We suggest that this inhibitor generates a good transition state analogue for this enzyme and interpret it in terms of mechanism accordingly.



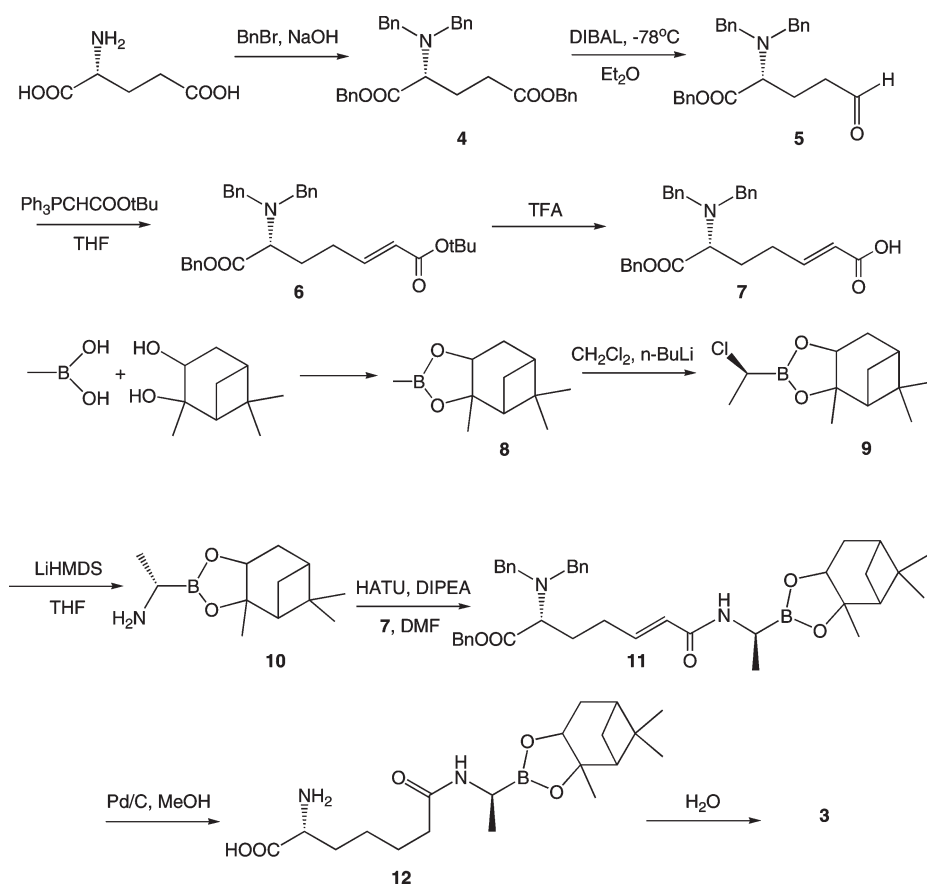
## MATERIALS AND METHODS

**Synthesis.** The synthesis of **3** is shown in outline in Scheme 2; the details are provided below.

*N,N*-Dibenzyl-D-glutamic Acid Dibenzy Ester (**4**) (40). To a solution of D-glutamic acid (5.0 g, 34 mmol, 1 equiv) in water (30 mL), together with potassium carbonate (18.8 g, 136 mmol, 4 equiv) and sodium hydroxide (2.75 g, 68 mmol, 2 equiv), heated under reflux, was added benzyl bromide (25 mL, 136 mmol) dropwise with stirring. The reaction was monitored by TLC (hexane/ethyl acetate), and upon completion, the reaction mixture was cooled to room temperature. The mixture was extracted with diethyl ether (3  $\times$  100 mL), and the combined organic layers were washed with water (50 mL) and brine (50 mL) and dried over magnesium sulfate. The ether was evaporated leaving a yellowish oil (13 g). It was purified by chromatography on silica gel (hexane:ethyl acetate, 7:1) yielding the product **4** as a colorless oil (10.5 g, 60% yield).  $^1\text{H NMR}$  ( $\text{CDCl}_3$ , 300 MHz)  $\delta$  2.1 (q,  $J$  = 7.5 Hz, 2H), 2.43, 2.56 (d quint,  $J$  = 9, 9 Hz, 2H), 3.47 (t,  $J$  = 7.5 Hz, 1H), 3.55, 3.93 (AB q,  $J$  = 13.5, 4H), 5.26 (AB q,  $J$  = 3 Hz, 2H), 5.20, 5.32 (AB q,  $J$  = 12 Hz, 2H), 7.25–7.46 (m, 20H).

*D*-4-(*N,N*-Dibenzylamino)-4-(benzyloxycarbonyl)butanal (**5**). To a stirred solution of **4** (3 g, 6 mmol, 1 equiv) in 30 mL of anhydrous diethyl ether under nitrogen atmosphere was added

Scheme 2



DIBAL (1 M in hexane, 6.5 mL, 1.1 equiv) slowly at  $-78^{\circ}\text{C}$ . The reaction was stirred for 15 min, and then water (0.3 mL) was added. The reaction was allowed to warm to room temperature and stirred additionally for 30 min after which it was dried over magnesium sulfate, filtered, and evaporated leaving a colorless gum, **5** (2.2 g), which was subjected to the next step without purification.  $^1\text{H NMR}$  ( $\text{CDCl}_3$ , 300 MHz)  $\delta$  1.21 (t,  $J = 7.8$  Hz, 2H), 2.3–2.5 (m, 2H), 3.35 (t,  $J = 7.2$  Hz, 1H), 3.52, 3.86 (AB q,  $J = 13.5$  Hz, 4H), 5.20, 5.26 (AB q,  $J = 10.8$  Hz, 2H), 7.2–7.5 (m, 15H), 9.58 (s, 1H).

*D*-6-(*N,N*-Dibenzylamino)-6-(benzyloxycarbonyl)-*trans*-hex-2-enoic Acid *tert*-Butyl Ester (**6**). To a stirred solution of **5** (2.0 g, 5 mmol, 1 equiv) in dry THF (20 mL) was added (*tert*-butoxycarbonylmethylene)triphenylphosphorane (2.6 g, 6.8 mmol, 1.2 equiv) at room temperature. The reaction was stirred for 1.5 h after which solvent was evaporated. The crude product was purified by chromatography on silica gel (hexane:ethyl acetate, 3:1), yielding the product **6** as a colorless oil (1.5 g, 60% yield).  $^1\text{H NMR}$  ( $\text{CDCl}_3$ , 300 MHz)  $\delta$  1.47 (s, 9H), 1.86 (m, 2H), 2.07 (m, 1H), 2.32 (m, 1H), 3.34 (t,  $J = 7.5$  Hz, 1H), 3.53, 3.87 (AB q,  $J = 13.5$  Hz, 4H), 5.19, 5.25 (AB q,  $J = 10.8$  Hz, 2H), 5.59 (d,  $J = 16$  Hz, 1H), 6.70 (quint,  $J = 7.2$  Hz, 1H), 7.2–7.4 (m, 15H).

*D*-6-(*N,N*-Dibenzylamino)-6-(benzyloxycarbonyl)-*trans*-hex-2-enoic Acid (**7**). The ester **6** (0.5 g, 1 mmol, 1 equiv) was dissolved in 5 mL of dichloromethane. To this solution, stirred in an ice bath, was added trifluoroacetic acid (6 mL) slowly. The reaction mixture was stirred for 1 h at room temperature after which solvent was evaporated. After the residue was dried under vacuum, the gummy product, **7**, was obtained (0.4 g, 90% yield).  $^1\text{H NMR}$  ( $\text{CDCl}_3$ , 300 MHz)  $\delta$  1.86 (m, 2H), 2.07 (m, 1H), 2.32

(m, 1H), 3.34 (t,  $J = 7.5$  Hz, 1H), 3.53, 3.87 (AB q,  $J = 13.5$  Hz, 4H), 5.19, 5.25 (AB q,  $J = 10.8$  Hz, 2H), 5.59 (d,  $J = 16$  Hz, 1H), 6.7 (quint,  $J = 7.2$  Hz, 1H), 7.2–7.4 (m, 15H). ES(+)MS  $m/z$  444.4 ( $M + 1$ ).

*Methylboronic Acid Pinanediol Ester (8)* (**41**). A mixture of methylboronic acid (1.0 g, 16.7 mmol, 1 equiv) and (–)-pinanediol (2.9 g, 16.7 mmol, 1 equiv) in diethyl ether (18 mL) was allowed to stir at room temperature over sodium sulfate for 1 h. This mixture was partitioned between a 10% aqueous solution of sodium carbonate (25 mL) and dichloromethane (25 mL). The organic solution was dried over sodium sulfate, evaporated, and distilled under vacuum (bp  $60^{\circ}\text{C}$ , 1 Torr), yielding the product **8** as a colorless oil (2.6 g, 80% yield).  $^1\text{H NMR}$  ( $\text{CDCl}_3$ , 300 MHz)  $\delta$  0.26 (s, 3H), 0.82 (s, 3H), 1.10 (d,  $J = 10.9$  Hz, 1H), 1.26 (s, 3H), 1.84–1.79 (m, 1H), 1.79 (s, 3H), 1.90–1.87 (m, 1H), 2.01 (t,  $J = 7$  Hz, 1H), 2.29 (m, 1H), 4.23 (dd,  $J = 8.7, 1.9$  Hz, 1H).

(*R*)-(Chloromethyl)boronic Acid Pinanediol Ester (**9**). This compound was prepared as described in ref 42. The crude material was purified by chromatography on silica gel (hexane:ethyl acetate, 24:1) and the product **9** obtained as a colorless oil (2.0 g, 80% yield).  $^1\text{H NMR}$  ( $\text{CDCl}_3$ , 300 MHz)  $\delta$  0.85 (s, 3H), 1.17 (d,  $J = 10.9$  Hz, 1H), 1.3 (s, 3H), 1.42 (s, 3H), 1.58 (d,  $J = 7.2$  Hz, 3H), 1.85–2.43 (m, 5H), 3.6 (q,  $J = 7.5$  Hz, 1H), 4.37 (dd,  $J = 1.9, 8.7$  Hz, 1H).

*D*-1-(Aminoethyl)boronic Acid Pinanediol Ester Hydrochloride (**10**). To a stirred solution of (*R*)-(chloromethyl)boronic acid pinanediol ester (2.0 g, 8.2 mmol, 1 equiv), in dry THF (20 mL) under an argon atmosphere at  $-100^{\circ}\text{C}$ , was added a 1 M solution in THF of lithium hexamethyldisilazane (9.3 mL, 1.13 equiv) dropwise down the cold wall. The reaction mixture was

allowed to warm to room temperature and stand for 24 h. The next reaction was carried out *in situ*. The reaction solution was cooled to  $-78\text{ }^{\circ}\text{C}$ , and 2 M hydrochloric acid in diethyl ether (12.3 mL, 3 equiv) was added dropwise down cold wall. The reaction mixture was allowed to warm to room temperature and then concentrated under reduced pressure to give a brown solid. This material was washed with ethyl acetate and dissolved in acetonitrile and the solution filtered. The filtrate was dried under reduced pressure to give a solid material, which was recrystallized from acetonitrile, affording the product **10** as a white solid (0.85 g, 40% yield).  $^1\text{H NMR}$  ( $\text{CDCl}_3$ , 300 MHz)  $\delta$  0.83 (s, 3H), 1.15 (d,  $J = 10.9$  Hz, 1H), 1.3 (s, 3H), 1.4 (s, 3H), 1.52 (d,  $J = 7.2$  Hz, 3H), 1.83–2.43 (m, 5H), 3.07 (br s, 1H), 4.39 (d,  $J = 8.5$  Hz, 1H), 8.23 (br s, 3H).

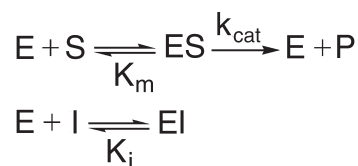
*D-1-[6-(N,N-Dibenzylamino)-6-(benzyloxycarbonyl)-trans-hex-2-enoylamino]ethylboronic Acid Pinanediol Ester (11)*. To a stirred solution of the acid **6** (300 mg, 0.68 mmol, 1 equiv) were added HATU (260 mg, 0.68 mmol, 1 equiv), diisopropylethylamine (230 mL, 1.36 mmol, 2 equiv) in dry DMF (10 mL), and the boronate ester **10** (180 mg, 0.75 mmol, 1.1 equiv) at  $0\text{ }^{\circ}\text{C}$ . The reaction mixture was then allowed to warm to room temperature and stirred overnight. Subsequently, it was concentrated under reduced pressure and the residue dissolved in ethyl acetate (20 mL). The ethyl acetate solution was washed with 0.1 N hydrochloric acid, saturated sodium bicarbonate, and brine and dried over magnesium sulfate. After evaporation of the organic solvent, the residual gum was further purified by chromatography on silica gel (3% MeOH/97%  $\text{CHCl}_3$ ), yielding the product **11** as a colorless foam (300 mg, 70% yield).  $^1\text{H NMR}$  ( $\text{CDCl}_3$ , 300 MHz)  $\delta$  0.86 (s, 3H), 1.2 (d,  $J = 7.5$  Hz, 3H), 1.28 (s, 3H), 1.44 (s, 3H), 1.75–2.4 (m, 13H), 2.93 (m, 1H), 3.35 (m, 1H), 3.54, 3.92 (AB q,  $J = 13.5$  Hz, 4H), 4.22 (d,  $J = 9$  Hz, 1H), 5.22 (AB q,  $J = 20$ , 10.8 Hz, 2H), 5.35 (d,  $J = 16$  Hz, 1H), 6.74 (quint,  $J = 7.2$  Hz, 1H), 7.24 (s, 5H), 7.26 (s, 5H), 7.28 (s, 5H).

*(D- $\alpha$ -Aminopimelylamino)-D-1-ethylboronic Acid Pinanediol Ester (12)*. The boronate ester **11** (200 mg, 0.30 mmol, 1 equiv) was dissolved in 10 mL of methanol, and 10% Pd on activated carbon (20 mg) was added. The hydrogenation reaction was carried out at 40 psi and at room temperature overnight. Pd/C was then removed by filtration, and methanol was evaporated, leaving a sticky gum. The residue was dissolved in anhydrous ethanol, and a white solid was precipitated by THF. This material, the product **12**, was washed with THF and hexane and dried under high vacuum (90 mg, 80% yield).  $^1\text{H NMR}$  ( $\text{CD}_3\text{OD}$ , 300 MHz)  $\delta$  0.88 (s, 3H), 1.11 (d,  $J = 7.2$  Hz, 3H), 1.3 (s, 3H), 1.35 (s, 3H), 1.59–2.43 (m, 14H), 2.58 (q,  $J = 7$  Hz, 1H), 3.74 (t,  $J = 6.5$  Hz, 1H), 4.14 (d,  $J = 8.5$  Hz, 1H). High-resolution ES(+)MS  $m/z$  381.2557 ( $M + 1$ ), calcd for  $\text{C}_{19}\text{H}_{34}\text{N}_2\text{O}_5\text{B}$  381.2561.

*(D- $\alpha$ -Aminopimelylamino)-D-1-ethylboronic Acid (3)*. The boronate ester **12** (20 mg, 0.05 mmol) was dissolved in water (10 mL) and extracted five times with dichloromethane (2 mL) over 24 h. The aqueous layer was freeze-dried, and the product **3** was obtained as a colorless glassy solid (7 mg, 57% yield).  $^1\text{H NMR}$  ( $\text{D}_2\text{O}$ , 300 MHz)  $\delta$  0.91 (d,  $J = 7$  Hz, 3H), 1.15–1.35 (m, 2H), 1.49–1.62 (m, 2H), 1.67–1.79 (m, 2H), 2.27 (t,  $J = 7.2$  Hz, 2H), 2.47 (q,  $J = 8.1$  Hz, 1H), 3.6 (t,  $J = 7.2$  Hz, 1H).

*Kinetics Studies*. An equilibrium constant for inhibition of the *Actinomadura* R39 DD-peptidase by the boronate **3** (0.05–1.0  $\mu\text{M}$ ) was obtained from steady-state competition experiments where *N*-phenylacetylglucyl-D-thiolactate (**43**) was employed as a chromophoric (245 nm) substrate (0.5 mM). The reaction conditions were 20 mM MOPS buffer, pH 7.50,  $25\text{ }^{\circ}\text{C}$ , and an

Scheme 3



enzyme concentration of 94.5 nM. Under these conditions, the  $K_m$  value of the substrate was  $38.4\text{ }\mu\text{M}$  (S. A. Adediran and R. F. Pratt, unpublished). Measurements of initial velocity vs boronate concentration were fitted to Scheme 3 by the Dynafit program (**44**) to obtain the  $K_i$  value directly.

*R39 DD-Peptidase Crystallography. Protein Purification and Crystallization*. The R39 DD-peptidase was expressed and purified as described previously (**45**). Crystals were grown at  $20\text{ }^{\circ}\text{C}$  by hanging drop vapor diffusion. Crystals were obtained by mixing  $4\text{ }\mu\text{L}$  of a  $25\text{ mg mL}^{-1}$  protein solution (also containing 5 mM  $\text{MgCl}_2$  and 20 mM Tris, pH 8),  $2\text{ }\mu\text{L}$  of well solution (2.0 M ammonium sulfate and 0.1 M MES, pH 6), and  $0.5\text{ }\mu\text{L}$  of 0.1 M  $\text{CoCl}_2$  solution. Crystals were soaked in  $9\text{ }\mu\text{L}$  of a solution containing 3.0 M ammonium sulfate and 0.1 M MES, pH 6, and  $0.1\text{ }\mu\text{L}$  of **3** (0.1 M).

*Data Collection, Structure Determination, and Refinement*. Data were collected at 100 K on an ADSC Q315r CCD detector at a wavelength of  $0.9797\text{ \AA}$  on beamline BM30A at the European Synchrotron Radiation Facility (ESRF, Grenoble, France). X-ray diffraction experiments were carried out under cryogenic conditions (100 K) after transferring the crystals into 45% glycerol and 1.8 M ammonium sulfate. Intensities were indexed and integrated using Mosflm (**46**). Data were scaled with SCALA of the CCP4 program suite (**47**). Refinement was carried out using REFMAC5 (**48**), TLS (**49**), and Coot (**50**). The structure of the R39 DD-peptidase bound to **3** was refined to  $2.4\text{ \AA}$  with  $R_{\text{cryst}}$  and  $R_{\text{free}}$  values of 20.0% and 26.2%, respectively. The ligand occupancy was refined as 1.0. Data statistics and refinement are summarized in Table 1.

## RESULTS AND DISCUSSION

Synthesis of the boronate inhibitor, **3**, was achieved according to Scheme 2. This molecule incorporates the peptidoglycan-mimetic D- $\alpha$ -aminopimelyl side chain, a specific binding motif for this enzyme (**13**, **51**), and a boronate reaction center. It was found to be a very powerful inhibitor of the R39 DD-peptidase, with an inhibition constant (assumed competitive in view of the structure of the inhibitor and supported subsequently by the structure of the complex, described below) of  $32 \pm 6\text{ nM}$ . The inhibition appeared to be fast and reversible under manual mixing conditions since no time-dependent phenomena were observed. The  $K_m$  value of **16** as a substrate is  $1.3\text{ }\mu\text{M}$  (**51**). Since deacylation is rate-determining at saturation (S. A. Adediran and R. F. Pratt, unpublished), this  $K_m$  value probably encompasses formation of the covalent acyl-enzyme intermediate, and thus the noncovalent dissociation constant must be greater than  $1\text{ }\mu\text{M}$ . The considerably tighter binding of **3** suggests that it may form a specific transition state analogue structure. This conclusion is supported by the crystal structure itself, discussed below. The boronate complexes of serine proteases (**52**) and serine  $\beta$ -lactamases (**32–34**) have generally been interpreted in this fashion.

Table 1: Data Collection and Refinement Statistics

data collection	
space group	$P2_1$
cell dimensions (Å, deg)	$a = 103.3, b = 91.6,$ $c = 106.9, \beta = 94.37$
resolution range (Å) <sup>a</sup>	33.1–2.4 (2.53–2.4)
no. of unique reflections	77588
$R_{\text{merge}}$ (%) <sup>a,b</sup>	9.5 (47.5)
redundancy <sup>a</sup>	3.6 (3.6)
completeness (%) <sup>a</sup>	99.7 (99.4)
$\langle I \rangle / \langle \sigma I \rangle$ <sup>a</sup>	9.7 (2.6)
refinement	
resolution range	32.4–2.4
no. of non-hydrogen protein atoms	14096
no. of water molecules	303
$R_{\text{cryst}}$ (%)	20.0
$R_{\text{free}}$ (%)	26.2
rms deviations from ideal stereochemistry	
bond lengths (Å)	0.009
bond angles (deg)	1.24
mean $B$ factor (all atoms) (Å <sup>2</sup> )	26.5
mean $B$ factor (ligand) (Å <sup>2</sup> )	28.1
Ramachandran plot	
most favored region (%)	91.7
additionally allowed regions (%)	7.7
generously allowed regions (%)	0.5
disallowed regions (%)	0.1
rmsd of C $\alpha$ atom with native structure (Å)	0.4 <sup>c</sup>
PDB code	2XDM

<sup>a</sup>Statistics for the highest resolution shell are given in parentheses.

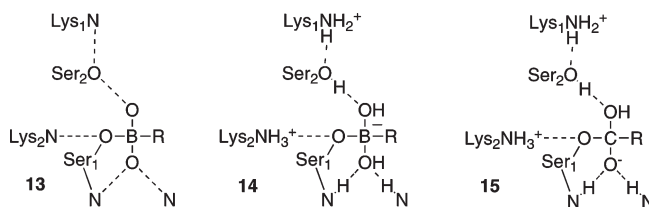
<sup>b</sup> $R_{\text{merge}} = \sum |I_i - I_m| / \sum I_i$ , where  $I_i$  is the intensity of the measured reflection and  $I_m$  is the mean intensity of all symmetry-related reflections. Numbers within parentheses are for the outer resolution shell. <sup>c</sup>Monomer B.

The overall fold of the R39 DD-peptidase complex with **3** is similar to that of the native enzyme structure (**53**) (rms deviation 0.4 Å). The asymmetric unit of the R39/**3** complex contains four protein molecules. The active sites of monomers B and C are each occupied by a molecule of **3**, whereas the active sites of monomers A and D are partly blocked by a symmetric molecule and are observed free of ligand. The rms difference between monomers B and C is 0.4 Å. The position of **3** in the active site of monomers B and C is similar, and the following description refers to monomer B. Electron density around the tetrahedral boronate moiety is well-defined.

The structure shows the boronate strongly bound to the enzyme active site (Figure 1). The aminopimelyl side chain is snugly accommodated in the specific binding pocket identified in the previous peptide and  $\beta$ -lactam structures (**13**). In particular, the amido group is held between its hydrogen bond partners, Asn 300 (NH<sub>2</sub>) and Thr 413 (C=O), the tetramethylene side chain abuts the hydrophobic side chains of Met 414 and Tyr 147, and the polar (ionic) carboxylate and ammonium termini are hydrogen bonded to Ser 415, Arg 351, and Asp 412. These interactions obviously define the specificity of the enzyme for motif **2**.

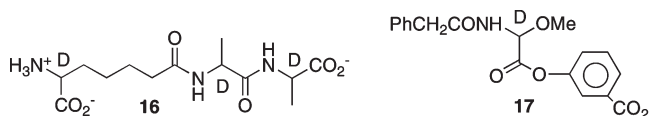
Closer to the reaction center, the D-methyl group is directed into a hydrophobic pocket in the surface (surrounded by Gly 148, Leu 349, and Met 414), as now seems likely to be typical of DD-peptidases (**26**, **54–56**); a larger side chain would not fit into this pocket. The boron is found in a tetrahedral, presumably anionic, configuration, covalently bound to the active site Ser 49 hydroxyl oxygen atom (bond length 1.44 Å). One boronate oxygen is firmly (2.9, 3.0 Å) hydrogen-bonded into the oxyanion hole (Ser 49 NH, Thr 413 NH) while the other is closely attended (2.7 Å) by the hydroxyl group of Ser 298. The latter is also close to Lys

410 N $\zeta$  (3.1 Å), as is Lys 52 N $\zeta$  to Ser 49 O $\beta$  (3.1 Å). A representation of this situation is shown as **13**.



The most likely incorporation of hydrogens into the putative hydrogen bonds of **13** yields **14**. If structure **14** is a direct analogue of a tetrahedral intermediate generated during the acyl transfer reaction of normal catalysis, then that intermediate would have structure **15**. In structures **13–15** and generally below, Ser 1 corresponds to the nucleophilic active site serine (Ser 49 in the R39 DD-peptidase), Lys 1, the lysine of the KT(S)G motif (Lys 410 in R39), Ser 2, the serine of the SXN motif (Ser 298), and Lys 2, the lysine of the SXXK motif (Lys 52). Although boronates (and phosphonates) have been interpreted in terms of the tetrahedral intermediate/transition states of both enzyme acylation and deacylation steps (**18**, **32–38**, **57**), because of the two hydroxyl groups on boron, boronates appear to most directly represent deacylation intermediates, generated by enzyme-catalyzed attack of water on the acyl-enzyme.

The presence of a sulfate ion, from the crystallization medium, in the crystal structure directly adjacent to the boronate moiety of the inhibitor is, however, interesting, in particular since one of its oxygen atoms is apparently hydrogen-bonded to the Thr 411 hydroxyl group. A sulfate at this position was also observed in the apoenzyme structure but was displaced by the  $\beta$ -lactam nitrocefin (**53**). This position approximates to the site where the carboxylate of the terminal D-alanine of a substrate might bind, probably also hydrogen-bonded to Thr 411 (**11–13**, **38**, **53**). Figure 2 shows a model of a tetrahedral intermediate derived from the excellent substrate **16** and directly built onto the boronate of the crystal structure. The substrate carboxylate can indeed occupy the same general space as the sulfate ion. In this way, to some degree at least, the boronate structure may also be seen as an acylation tetrahedral intermediate analogue.



The deacylation tetrahedral intermediate **15** might then be generated by mechanism a, b, or c (Scheme 4) and break down to products by either d, e, or f. In mechanism a, nucleophilic attack of water on the acyl-enzyme is assisted by Lys 2 acting as a general base although proton transfer is indirect via Ser 2. In the alternative mechanism b, water attack is facilitated by Lys 1 as a general base, again indirectly via Ser 2. Direct action of Lys 2 as a general base is the centerpiece of mechanism c, where Ser 2 and Lys 1 appear to have only spectator or electrostatic roles.

Breakdown of the tetrahedral intermediate also has three alternative paths, d, e, and f, which are symmetrical analogues of a, b, and c, respectively. In d, the general acid catalyst facilitating departure of Ser 1 is Lys 2, whereas in e, it is the protonated

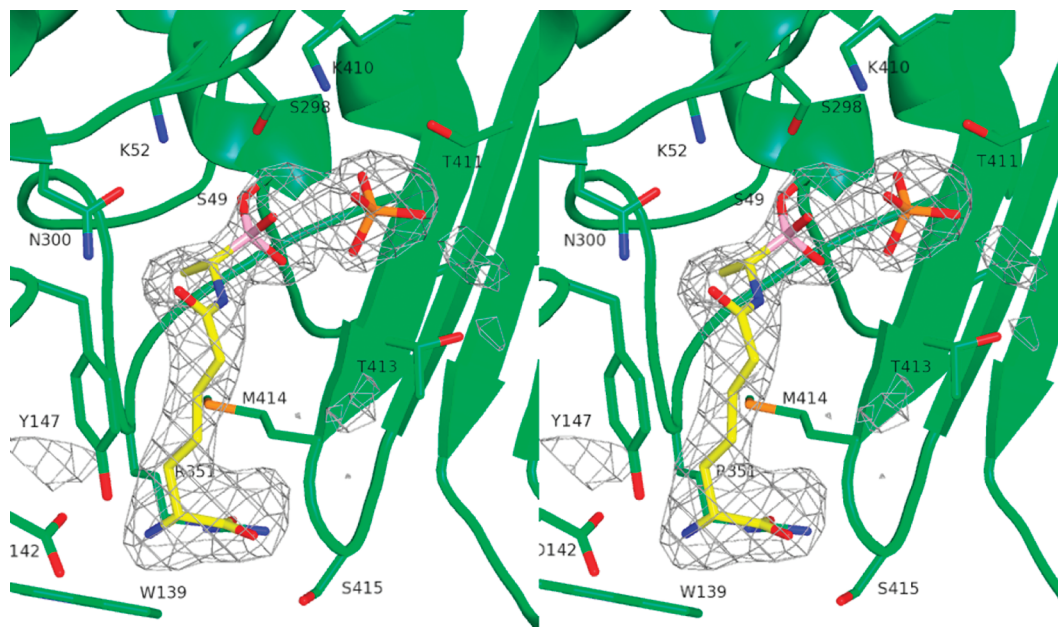


FIGURE 1: Crystal structure of the R39 DD-peptidase in complex with the specific boronate **3**. In this stereoview, the electron density is a  $|F_o| - |F_c|$  difference map calculated from the final coordinates of the model refined in the absence of ligand. The resulting positive density is shown with brown hatching and is contoured at  $2.5\sigma$ . The protein backbone and secondary structure are in green, and the boronate is in yellow. Heteroatoms are red (oxygen), blue (nitrogen), orange (sulfur), and pink (boron). Also shown is a sulfate of crystallization bound at the active site. This figure was generated using PYMOL ([www.pymol.sourceforge.net](http://www.pymol.sourceforge.net)).

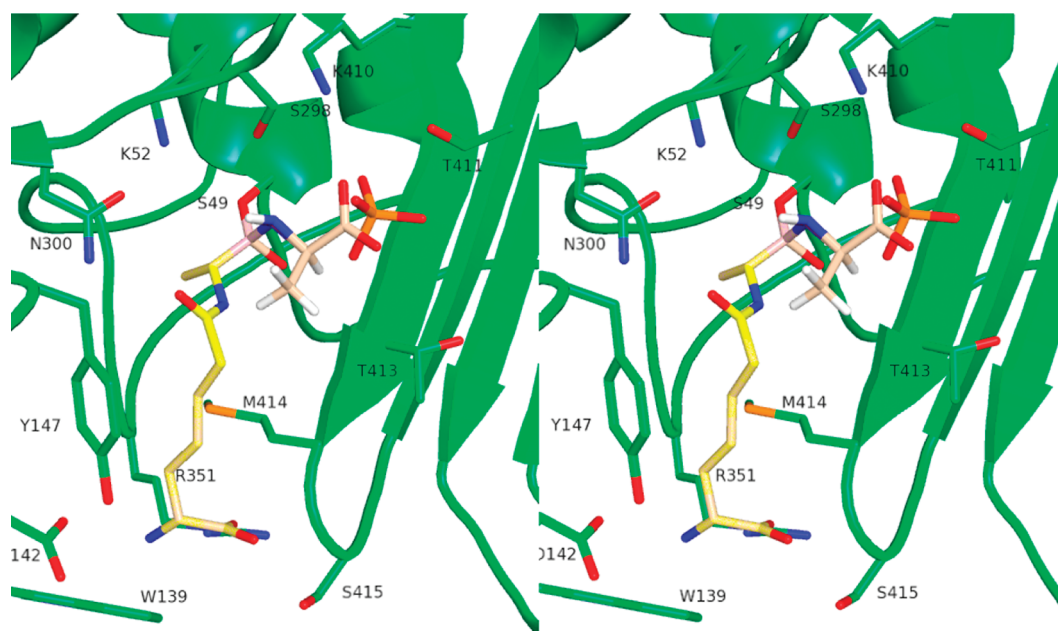


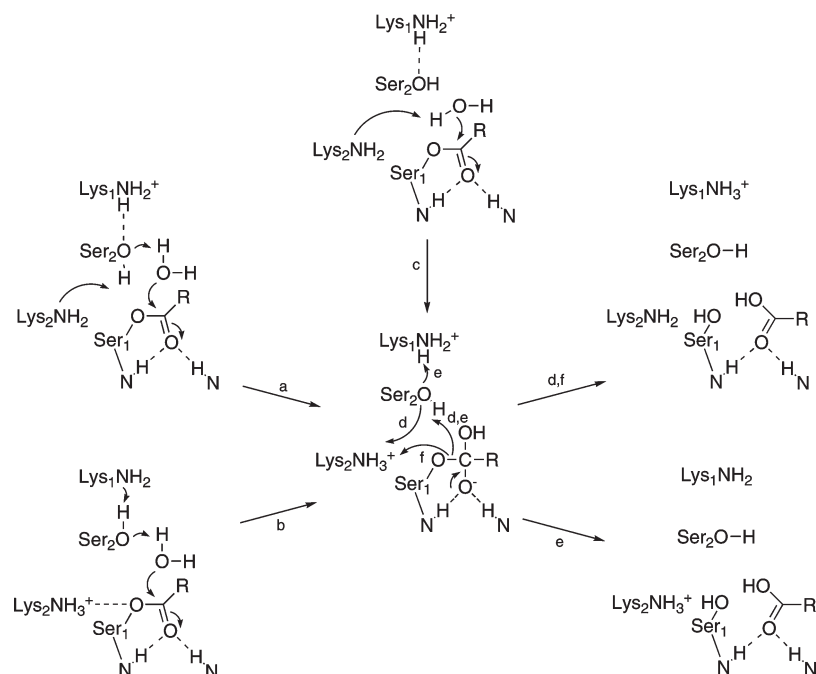
FIGURE 2: A model of the tetrahedral intermediate generated on reaction of the enzyme with the substrate **16**. The sulfate of crystallization is also shown. The model was constructed by replacement of the appropriate boronate oxygen in the structure of Figure 1 with a D-alanine leaving group (salmon) and shows the overlap between the leaving group carboxylate and the sulfate anion. The other colors are as for Figure 1. This figure was generated using PYMOL ([www.pymol.sourceforge.net](http://www.pymol.sourceforge.net)).

Lys 1, both acting by way of Ser 2. In mechanism f, Lys 2 acts alone as a general acid. With the assumption of mechanistic symmetry, the simplest possibility, these mechanisms can then be extrapolated to analogous mechanisms of acylation (Scheme 5, where L is the leaving group, D-Ala, in a carboxypeptidase or transpeptidase reaction).

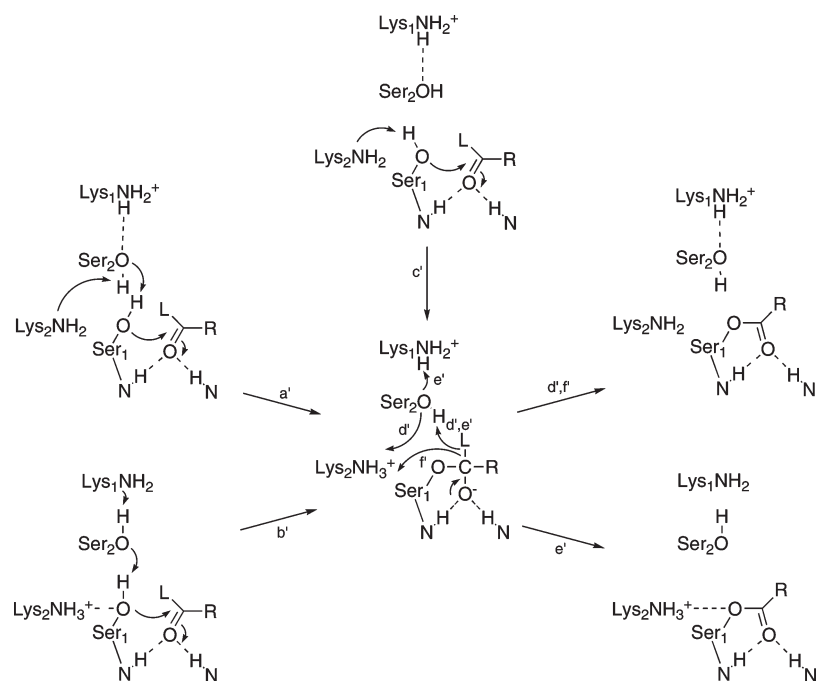
Of these mechanisms, almost all have been previously proposed at one time or another for one reason or another. In particular, the combination of a' and d' in acylation, and thus a and d in deacylation, has been seriously discussed (15). The combination

of a (a') and e (e') has also been suggested by Nicola et al. (18) and Diaz et al. (21). To some extent at least, the distinction between mechanisms a (a') and b (b') centers around the relative  $pK_a$  values of Lys 1 and Lys 2 and thus relates to the pH-rate profiles of various DD-peptidases. This issue has been much discussed (see ref 8, for example, for a review of the situation). In the present authors' opinion, the currently available evidence probably favors a lower  $pK_a$  for Lys 2, but the issue is still open, particularly with respect to the lysine  $pK_a$ s in the various intermediate complexes.

Scheme 4



Scheme 5



One mechanism, specific to acylation, and involving the substrate carboxyl group as a member of the proton donation path to the leaving group, has also been considered (20, 21). Apart from the clear, although not decisive, defect that this mechanism could not apply to deacylation, is the observation that molecules such as **17**, where the carboxylate is very differently placed with respect to the scissile bond, can be excellent substrates of the R39 DD-peptidase (54). This observation suggests that such participation by the substrate carboxylate is not essential to facilitate acylation.

One pathway, distinguished by its simplicity and its similarity to many protease mechanisms, is the combination of c and f in deacylation (Scheme 4) along with c' and f' in acylation (Scheme 5).

This employs Lys 2 as the sole general acid/base catalyst and is supported by computational results from Zhang et al. (22). The downside of this proposal has always been the Ser 2, Lys 1 combination, which in this mechanism appears to play no obvious role. This dyad has previously been observed in many crystal structures of covalent DD-peptidase/ $\beta$ -lactam complexes, in close association with the ligand. Some examples are found in refs (58–61). In the current structure, we find Ser 2 apparently tightly hydrogen-bonded to the boronate “leaving group” oxygen. If the boronate is indeed an analogue of a high-energy intermediate, it seems unlikely that Ser 2 is not part of the mechanism. An issue that clouds the computational study referred to above (22) is that the system studied was *E. coli* PBP5. This DD-peptidase is unusual

and unique (except for its close homologue *E. coli* PBP6 (62)) in having a broadened active site, at least in the crystal structure. This property is illustrated, for example, by the larger than usual distance between C $\alpha$  of Ser 2 (Ser 298) and C $\alpha$  of Gly 413 (of the KS(T)G motif) (13) which leads to a considerable separation between the Ser 1 and Ser 2 side chains. In the crystal structure of a nonspecific boronate complex with PBP5 (18), the active site breadth has decreased to around the average value (13), suggesting that the PBP5 active site may undergo a significant conformational change on reaction with a substrate. Although Zhang et al. (22) were aware of this problem and apparently attempted to address it, there remains uncertainty as to whether they succeeded. Certainly, their computed intermediates appear to retain the original separation of Ser 1 and Ser 2.

The present structure of Figure 1 therefore is probably best interpreted, taking into account all currently available evidence, in terms of a catalytic mechanism of deacylation represented by the sequences a and d, and thus, assuming symmetry between acylation and deacylation, a' followed by d' in acylation. Only the uncertainty of the actual pK<sub>s</sub> of Lys 1 and Lys 2 seems to remain as an issue that may affect this conclusion. It is interesting that a popular mechanism of acylation of class A  $\beta$ -lactamases follows a similar path involving the homologue of Ser 2 in proton transfer to the leaving group (27, 63, 64).

The strong affinity of 3 for the R39 DD-peptidase suggests that specific boronates may generally be very powerful DD-peptidase inhibitors and thus, possibly, antibiotics. Gutheil has previously raised this possibility (65). For it to be achieved, however, the specificity puzzle of high molecular weight PBPs (7, 8, 13) will have to be solved.

## ACKNOWLEDGMENT

We thank the staff of beamline FIP/BM30a at ESRF for assistance in X-ray data collection. We also thank R. Herman for expert work in protein crystallization.

## REFERENCES

- Vollmer, W., and Bertsche, U. (2007) Murein (peptidoglycan) structure, architecture and biosynthesis in *E. coli*. *Biochim. Biophys. Acta* 1778, 1714–1734.
- Payne, D. J., Gwynn, M. N., Holmes, D. J., and Pompliano, D. L. (2007) Drugs for bad bugs: confronting the challenges of antibacterial discovery. *Nat. Rev. Drug Discovery* 6, 29–39.
- Ghuysen, J.-M., Frère, J.-M., Leyh-Bouille, M., Coyette, J., Dusart, J., and Nguyen-Distèche, M. (1979) Use of model enzymes in the determination of the mode of action of penicillins and  $\Delta^3$ -cephalosporins. *Annu. Rev. Biochem.* 48, 73–101.
- Waxman, D. J., and Strominger, J. L. (1983) Penicillin-binding proteins and the mechanism of action of  $\beta$ -lactam antibiotics. *Annu. Rev. Biochem.* 52, 825–869.
- Ghuysen, J.-M. (1991) Serine  $\beta$ -lactamases and penicillin-binding proteins. *Annu. Rev. Microbiol.* 45, 35–67.
- Macheboeuf, P., Contreras-Martel, C., Job, V., Dideberg, O., and Dessen, A. (2006) Penicillin-binding proteins: key players in bacterial cell cycle and drug resistance processes. *FEMS Microbiol. Rev.* 30, 673–691.
- Sauvage, E., Kerff, F., Terrak, M., Ayala, J. R., and Charlier, P. (2008) The penicillin-binding proteins: structure and role in peptidoglycan biosynthesis. *FEMS Microbiol. Rev.* 32, 234–258.
- Josephine, H. R., Charlier, P., Davies, C., Nicholas, R. A., and Pratt, R. F. (2006) Reactivity of penicillin-binding proteins with peptidoglycan-mimetic  $\beta$ -lactams: what's wrong with these enzymes? *Biochemistry* 45, 15873–15883.
- Pratt, R. F. (2008) Substrate specificity of bacterial DD-peptidases (penicillin-binding proteins). *Cell. Mol. Life Sci.* 65, 2138–2155.
- Anderson, J. W., and Pratt, R. F. (2000) Dipeptide binding to the extended active site of the *Streptomyces* R61 D-alanyl-D-alanine-peptidase: the path to a specific substrate. *Biochemistry* 39, 12200–12209.
- McDonough, M. A., Anderson, J. W., Silvaggi, N. R., Pratt, R. F., Knox, J. R., and Kelly, J. A. (2002) Structures of two kinetic intermediates reveal species specificity of penicillin-binding proteins. *J. Mol. Biol.* 322, 111–122.
- Silvaggi, N. R., Josephine, H. R., Kuzin, A. P., Nagarajan, R., Pratt, R. F., and Kelly, J. A. (2005) Crystal structures of complexes between the R61 DD-peptidase and peptidoglycan-mimetic  $\beta$ -lactams: a non-covalent complex with a “perfect penicillin”. *J. Mol. Biol.* 345, 521–533.
- Sauvage, E., Powell, A. J., Heilemann, J., Josephine, H. R., Charlier, P., Davies, C., and Pratt, R. F. (2008) Crystal structures of complexes of bacterial DD-peptidases with peptidoglycan-mimetic ligands: the substrate specificity puzzle. *J. Mol. Biol.* 381, 383–393.
- Morlot, C., Pernot, C., LeGouellec, A., DiGiulmi, A. M., Vernet, T., Dideberg, O., and Dessen, A. (2005) Crystal structure of a peptidoglycan synthesis regulatory factor (PBP 3) from *Streptococcus pneumoniae*. *J. Biol. Chem.* 280, 15984–15991.
- Sauvage, E., Duez, C., Herman, R., Kerff, F., Petrella, S., Anderson, J. W., Adediran, S. A., Pratt, R. F., Frère, J.-M., and Charlier, P. (2007) Crystal structure of the *Bacillus subtilis* penicillin-binding protein 4a and its complex with a peptidoglycan-mimetic peptide. *J. Mol. Biol.* 371, 528–539.
- Stefanova, M. E., Tomberg, J., Davies, C., Nicholas, R. A., and Gutheil, W. G. (2006) Overexpression and enzymatic characterization of *Neisseria gonorrhoeae* penicillin-binding protein 4. *Eur. J. Biochem.* 271, 23–32.
- Rhazi, N., Charlier, P., Dehareng, D., Engher, D., Vermeire, M., Frère, J.-M., Nguyen-Distèche, M., and Fonze, E. (2003) Catalytic mechanism of the *Streptomyces* K15 DD-transpeptidase/penicillin-binding protein probed by site-directed mutagenesis and structural analysis. *Biochemistry* 42, 2895–2906.
- Nicola, G., Peddi, S., Stefanova, M., Nicholas, R. A., Gutheil, W. G., and Davies, C. (2005) Crystal structure of *Escherichia coli* penicillin-binding protein 5 bound to a tripeptide boronic acid inhibitor: a role for Ser 110 in deacylation. *Biochemistry* 44, 8207–8217.
- Thomas, B., Wang, Y., and Stein, R. (2001) Kinetic and mechanistic studies of penicillin-binding protein 2x from *Streptococcus pneumoniae*. *Biochemistry* 40, 15811–15823.
- Oliva, M., Dideberg, O., and Field, M. J. (2003) Understanding the acylation mechanisms of active site serine penicillin-recognizing proteins: a molecular dynamics simulation study. *Proteins: Struct., Funct., Genet.* 52, 88–100.
- Díaz, N., Sordo, T. L., and Suárez, D. (2005) Insights into the base catalysis exerted by the DD-transpeptidase from *Streptomyces* K15: a molecular dynamics study. *Biochemistry* 44, 3225–3240.
- Zhang, W., Shi, Q., Meroueh, S. O., Vakulenko, S. B., and Mobashery, S. (2007) Catalytic mechanism of penicillin-binding protein 5 of *Escherichia coli*. *Biochemistry* 46, 10113–10121.
- Golemi-Kotra, D., Meroueh, S. O., Kim, C., Vakulenko, S. B., Bulychev, A., Stemmler, A. J., Stemmler, T. L., and Mobashery, S. (2004) The importance of a critical protonation state and the fate of the catalytic steps in class A  $\beta$ -lactamases and penicillin-binding proteins. *J. Biol. Chem.* 279, 7652–7664.
- Gherman, B. F., Goldberg, S. D., Cornish, V. W., and Freisner, R. A. (2004) Mixed quantum mechanical/molecular mechanics (QM/MM) study of the deacylation reaction in a penicillin-binding protein (PBP) versus in a class C  $\beta$ -lactamase. *J. Am. Chem. Soc.* 126, 7652–7664.
- Tipper, D. J., and Strominger, J. L. (1965) Mechanism of action of penicillins: a proposal based on their structural similarity to acyl-D-alanyl-D-alanine. *Proc. Natl. Acad. Sci. U.S.A.* 54, 1133–1141.
- Pratt, R. F. (2002) Functional evolution of the serine  $\beta$ -lactamase active site. *J. Chem. Soc., Perkin Trans. 2*, 851–861.
- Matagne, A., Dubus, A., Galleni, M., and Frère, J.-M. (1999) The  $\beta$ -lactamase cycle: a tale of selective pressure and bacterial ingenuity. *Nat. Prod. Rep.* 16, 1–19.
- Minasov, G., Wang, X., and Shoichet, B. K. (2002) An ultrahigh resolution structure of TEM-1  $\beta$ -lactamase suggests a role for Glu 166 as the general base in acylation. *J. Am. Chem. Soc.* 124, 5333–5340.
- Nukaga, M., Mayama, M., Hujer, A. M., Bonomo, R. A., and Knox, J. R. (2003) Ultra high resolution structure of a class A  $\beta$ -lactamase: on the mechanism and specificity of the extended-spectrum SHV-2 enzyme. *J. Mol. Biol.* 328, 289–301.
- Díaz, N., Sordo, T. L., Merz, K. M., Jr., and Suárez, D. (2003) Insights into the acylation mechanism of class A  $\beta$ -lactamases from molecular dynamics simulations of the TEM-1 enzyme complexed with benzylpenicillin. *J. Am. Chem. Soc.* 125, 672–684.
- Hermann, J. C., Hensen, C., Ridder, L., Mulholland, A. J., and Höltje, H.-D. (2005) Mechanisms of antibiotic resistance: QM/MM

- modeling of the acylation reaction of a class A  $\beta$ -lactamase with benzylpenicillin. *J. Am. Chem. Soc.* 127, 4454–4465.
32. Strynadka, N. C. J., Martin, R., Jensen, S. E., Gold, M., and Jones, J. B. (1996) Structure-based design of a potent transition state analogue for TEM-1  $\beta$ -lactamase. *Nat. Struct. Biol.* 3, 688–695.
  33. Powers, R. A., Caselli, E., Focia, P. J., Prati, F., and Shoichet, B. K. (2001) Structures of ceftazidime and its transition state analogue in complex with AmpC  $\beta$ -lactamase: implications for resistance mutations and inhibitor design. *Biochemistry* 40, 9207–9214.
  34. Morandi, F., Caselli, E., Morandi, S., Focia, P. J., Blázquez, J., Shoichet, B. K., and Prati, F. (2003) Nanomolar inhibitors of AmpC  $\beta$ -lactamase. *J. Am. Chem. Soc.* 125, 685–695.
  35. Chen, C. C. H., Rahil, J., Pratt, R. F., and Herzberg, O. (1993) Structure of a phosphonate-inhibited  $\beta$ -lactamase. An analog of the tetrahedral transition state/intermediate of  $\beta$ -lactam hydrolysis. *J. Mol. Biol.* 234, 165–178.
  36. Lobkovsky, E., Billings, E. M., Moews, P. C., Rahil, J., Pratt, R. F., and Knox, J. R. (1994) Crystallographic structure of a phosphonate derivative of the *Enterobacter cloacae* P99 cephalosporinase: mechanistic interpretation of a  $\beta$ -lactamase transition state analog. *Biochemistry* 33, 6762–6772.
  37. Maveyraud, L., Pratt, R. F., and Samama, J.-P. (1998) Crystal structure of an acylation transition state analog of the TEM-1  $\beta$ -lactamase. Mechanistic implications for class A  $\beta$ -lactamases. *Biochemistry* 37, 2622–2628.
  38. Silvaggi, N. R., Anderson, J. W., Brinsmade, S. A., Pratt, R. F., and Kelly, J. A. (2003) The crystal structure of phosphonate-inhibited D-Ala-D-Ala peptidase reveals an analogue of a tetrahedral transition state. *Biochemistry* 42, 1199–1208.
  39. Inglis, S. R., Zervosen, A., Woon, E. C. Y., Gerards, T., Teller, N., Fischer, D. S., Luxen, A., and Schofield, C. J. (2009) Synthesis and evolution of 3-(dihydroxy-boryl) benzoic acids as DD-carboxypeptidase R39 inhibitors. *J. Med. Chem.* 52, 6097–6106.
  40. Rodriguez, M., and Taddei, M. (2005) A simple procedure for the transformation of L-glutamic acid into the corresponding  $\gamma$ -aldehyde. *Synthesis* 3, 493–495.
  41. Maurer, K. W., and Armstrong, R. W. (1996) Synthesis of the C1-C21 fragment of the serine/threonine phosphatase inhibitor tautomycin. *J. Org. Chem.* 61, 3106–3116.
  42. Matteson, D. S., Sadhu, K. M., and Peterson, M. L. (1986) 99% chirally selective synthesis via pinanediol boronic esters: insect pheromones, diols, and an amino alcohol. *J. Am. Chem. Soc.* 108, 810–819.
  43. Xu, Y., Soto, G., Adachi, H., van der Linden, M. P. G., Keck, W., and Pratt, R. F. (1994) Relative specificities of a series of  $\beta$ -lactam-recognizing enzymes towards the side chains of penicillins and of acyclic thioldepsipeptides. *Biochem. J.* 302, 851–856.
  44. Kuzmic, P. (1996) Program DYNAFIT for the analysis of enzyme kinetic data: application to HIV proteinase. *Anal. Biochem.* 237, 260–273.
  45. Granier, B., Duez, C., Lepage, S., Englebort, S., Dusart, J., Dideberg, O., Van Beeumen, J., Frère, J.-M., and Ghuysen, J.-M. (1992) Primary and predicted secondary structures of the *Actinomadura* R39 extracellular DD-peptidase, a penicillin-binding protein (PBP) related to *Escherichia coli* PBP4. *Biochem. J.* 282, 781–788.
  46. Leslie, A. G. W. (1991) Molecular data processing. *Crystallogr., Comput.* 5, 50–61.
  47. CCP4 (1994) The CCP4 suite: programs for protein crystallography. *Acta Crystallogr., Sect. D: Biol. Crystallogr.* 50, 760–763.
  48. Murshudov, G. N., Vagin, A. A., and Dodson, E. J. (1997) Refinement of macromolecular structures by the maximum-likelihood method. *Acta Crystallogr. D* 53, 240–255.
  49. Painter, J., and Merritt, E. A. (2006) Optimal description of a protein structure in terms of multiple groups undergoing TLS motion. *Acta Crystallogr., Sect. D: Biol. Crystallogr.* 62, 439–50.
  50. Emsley, P., and Cowtan, K. (2004) Coot: model-building tools for molecular graphics. *Acta Crystallogr., Sect. D: Biol. Crystallogr.* 60, 2126–2132.
  51. Anderson, J. W., Adediran, S. A., Charlier, P., Nguyen-Distèche, M., Frère, J.-M., Nicholas, R. A., and Pratt, R. F. (2003) On the substrate specificity of bacterial DD-peptidases: evidence from two series of peptidoglycan-mimetic peptides. *Biochem. J.* 373, 949–955.
  52. Tulinsky, A., and Blevins, R. A. (1987) Structure of a tetrahedral transition state complex  $\gamma$ -chymotrypsin dimer at 1.8 Å resolution. *J. Biol. Chem.* 262, 7737–7743.
  53. Sauvage, E., Herman, R., Petrella, S., Duez, C., Bouillenne, F., Frère, J.-M., and Charlier, P. (2005) Crystal structure of the *Actinomadura* R39 DD-peptidase reveals new domains in penicillin-binding proteins. *J. Biol. Chem.* 280, 31249–31256.
  54. Bernstein, N. J., and Pratt, R. F. (1999) On the importance of a methyl group in  $\beta$ -lactamase evolution: free energy profiles and molecular modeling. *Biochemistry* 38, 10499–10510.
  55. Adediran, S. A., Zhang, Z., Nukaga, M., Palzkill, T., and Pratt, R. F. (2005) The D-methyl group in  $\beta$ -lactamase evolution: evidence from the Y221G and GC1 mutants of the class C  $\beta$ -lactamase of *Enterobacter cloacae* P99. *Biochemistry* 44, 7543–7552.
  56. Adediran, S. A., Cabaret, D., Flavell, R. R., Sammons, J. A., Wakselman, M., and Pratt, R. F. (2006) Synthesis and  $\beta$ -lactamase reactivity of  $\alpha$ -substituted phenacetates. *Bioorg. Med. Chem.* 14, 7023–7033.
  57. Chen, Y., Shoichet, B., and Bonnet, R. (2005) Structure, function, and inhibition along the reaction coordinate of CTX-M  $\beta$ -lactamases. *J. Am. Chem. Soc.* 127, 5423–5434.
  58. Gordon, E., Mouz, N., Duée, E., and Dideberg, O. (2000) The crystal structure of the penicillin-binding protein 2x from *Streptococcus pneumoniae* and its acyl-enzyme form: implication in drug resistance. *J. Mol. Biol.* 299, 477–485.
  59. Lim, D., and Strynadka, N. C. J. (2002) Structural basis for the  $\beta$ -lactam resistance of PBP2a from methicillin-resistant *Staphylococcus aureus*. *Nat. Struct. Biol.* 9, 870–876.
  60. Contreras-Martel, C., Job, V., Di Giulmi, A. M., Vernet, T., Dideberg, O., and Dessen, A. (2006) Crystal structure of penicillin-binding protein 1a (PBP1a) reveals a mutational hotspot implicated in  $\beta$ -lactam resistance in *Streptococcus pneumoniae*. *J. Mol. Biol.* 355, 684–696.
  61. Kishida, H., Unzai, S., Roper, D. I., Lloyd, A., Park, S.-Y., and Tame, J. R. H. (2006) Crystal structure of penicillin binding protein 4 (dac B) from *Escherichia coli*, both in the native form and covalently linked to various antibiotics. *Biochemistry* 45, 783–792.
  62. Chen, Y., Zhang, W., Shi, Q., Hesk, D., Lee, M., Mobashery, S., and Shoichet, B. K. (2009) Crystal structure of penicillin-binding protein 6 from *Escherichia coli*. *J. Am. Chem. Soc.* 131, 14345–14354.
  63. Drawz, S. M., and Bonomo, R. A. (2010) Three decades of  $\beta$ -lactamase inhibitors. *Clin. Microbiol. Rev.* 23, 160–201.
  64. Meroueh, S. O., Fisher, J. F., Schlegel, H. B., and Mobashery, S. (2005) Ab initio QM/MM study of class A  $\beta$ -lactamase acylation: dual participation of Glu 166 and Lys 73 in a concerted base promotion of Ser 70. *J. Am. Chem. Soc.* 127, 15397–15407.
  65. Gutheil, W. G. (1996) Antibacterial peptidomimetics and their preparation, U.S. Patent 5574017.